Journal of Materials Education Vol.22 (4-6): 107-129 (2000)

EPOXY THERMOSETS AND THEIR APPLICATIONS. II. THERMAL ANALYSIS

Bryan Bilyeu[1], Witold Brostow[1] and Kevin P. Menard[2]

[1]Department of Materials Science, University of North Texas, TX 76205-5310, USA
[2]Perkin-Elmer LLC, 50 Danbury Road, Wilton, CT 06897, USA

ABSTRACT

Since the curing process of an epoxy thermoset is thermally-activated and temperature dependent, thermal analysis is the most common method to monitor the process. In addition, many common temperature-dependent properties like heat capacity and modulus change with the degree of cure or extent of cross-linking. Common thermal analysis techniques which are applicable to the study of thermoset cure are reviewed, specifically differential scanning calorimetry (DSC and TMDSC), thermomechanical and dynamic mechanical analysis (TMA and DMA), thermally stimulated depolarization (TSD), and thermogravimetric analysis (TGA).

Keywords: *Epoxy thermoset; thermal analysis*

1. INTRODUCTION

The basic structure and properties unique to epoxies have been described in a previous paper,[1] so the techniques which characterize the changes in properties in an epoxy during curing are discussed.

In the most basic sense, thermal analysis is the study of the state or changes of state of a material in terms of temperature. A qualitative understanding of changes of properties of materials with temperature has existed since the first pottery and bricks were fired and the first bread was baked, with evidence depicted graphically in numerous carvings and drawings, including well preserved Egyptian excavations[2] depicting a balance and fire. However, quantitative thermal analysis required measurable quantities. The first and most important of these was thermometry, introduced in 17th century Florence.[3] With temperature, properties like heat capacity could shed light onto the intrinsic properties of materials. Differential thermal analysis was introduced in the late 1800's by Le Chatelier,[4] Nernst[5] introduced the thermobalance in 1903, and other techniques as well as improvements in existing techniques followed quickly.[6]

The International Confederation for Thermal Analysis and Calorimetry (ICTAC) defined thermal analysis as "a group of techniques in which a property of the sample is monitored

against time or temperature while the temperature of the sample, in a specified atmosphere, is programmed."[7] This definition was adopted by the International Union of Pure and Applied Chemistry (IUPAC) and the American Society for Testing and Materials (ASTM).[8]

2. HEAT OF REACTION

Due to the high potential energy of the ring-strained epoxide groups in the uncured resin, there is a large Gibbs function difference associated with the ring-opening reaction. Since the Gibbs function change ΔG is expressed in the form of both enthalpic ΔH and entropic ΔS contributions, the reaction is called exergenic.[9] Although structural changes will result in a significant entropy change, the enthalpy change is the dominant effect. That change in this case results in the evolution of thermal energy or heat, an exothermic reaction. Since the opening of the epoxide rings have much higher energy (and enthalpy) differences than the other reactions, the amount of heat evolved and the rate of evolution will correspond to the number of epoxide groups reacting and the rate of the reaction.

Reactions which generate heat are studied by calorimetry. Many types of calorimeters exist although only a few are appropriate for polymerization reactions. Early studies of epoxy polymerization used differential thermal analysis (DTA), which monitors temperature differences between the sample and a reference, and adiabatic calorimetry, which monitors the temperature of a thermally isolated system. However, these techniques have low sensitivities and many limitations.[10] The current standard technique for quantitative evaluation is the measurement of the change in enthalpy using Differential Scanning Calorimetry (DSC) since the heat flow during a constant pressure reaction is defined as the change in enthalpy of the system.

Two types of DSCs are available, a heat-flux

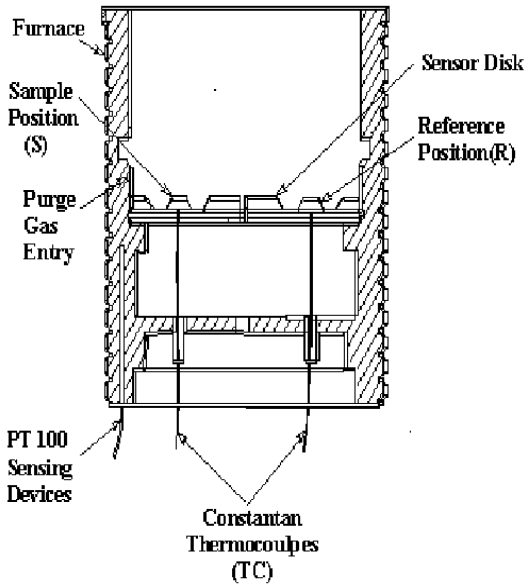

Fig.1. Schematic of a heat-flux DSC.

DSC (based on the Boersma[11] DTA design) and a power-compensation DSC. The heat-flux DSC,[12] shown in Figure 1, measures the difference in temperature between a sample and reference heated at a programmed rate in a common oven using thermocouples attached to the bottom of the sample holders. The power-compensation DSC,[13,14] in Figure 2, employs separate heating elements and thermocouples for sample and reference applying separate currents to the heaters to maintain a null difference in the temperature.

Both types of DSC instruments generate plots of heat flow as a function of the programmed temperature. However, due to the difference in measurement techniques, the heat flow ordinate value is calculated differently. Since the heat-flux DSC measures the temperature difference between the sample and reference cells, calculation of the heat flow requires an accurate temperature and sample dependent thermal resistance value of the system as a proportionality factor.[15] The power-compensation DSC also requires a thermal resistance value; however, that value represents the heating elements, not the entire system, and is constant over a wide operating temperature

range.[16,17] The power-compensation DSC maintains the programmed temperature ramp in both sample and reference, ensuring much better temperature control in the sample.[18]

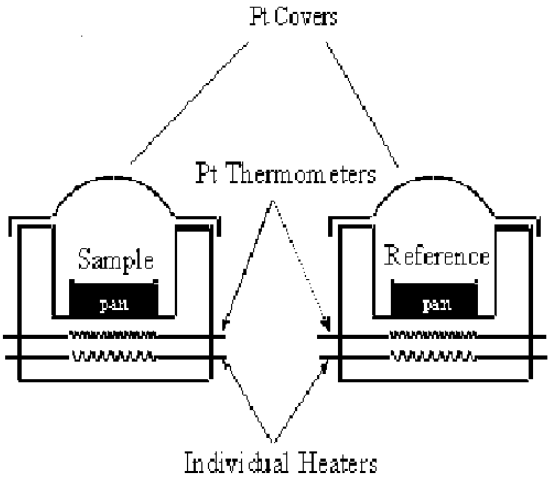

Fig.2. Schematic of power-compensation DSC.

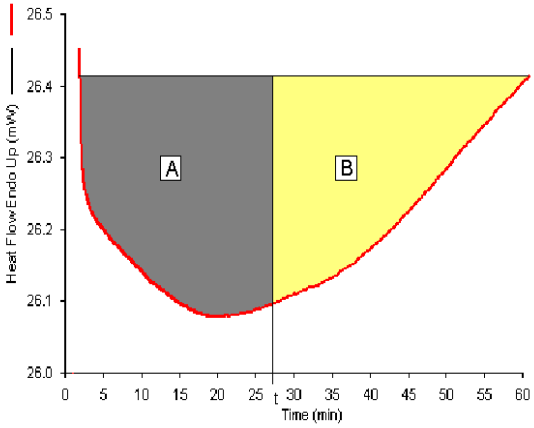

Fig. 3. An example of a DSC thermogram showing the portion of the total reaction, as measured by the enthalpic exotherm, reacted at time t.

To determine the extent of a curing reaction or the degree of cure α the change in enthalpy is compared to the total change in enthalpy of the complete reaction, as illustrated in Figure 3, that is

$$\alpha = \Delta H/\Delta H_{total} \qquad (1)$$

Alternatively, the difference between the total and any residual enthalpy changes can be compared to the total, where ΔH in Equation 1 would be replaced by $(\Delta H_{total} - \Delta H_{resid})$.[19] Generally, the total change in enthalpy is determined using a slow temperature ramp from a low temperature to a temperature just below the onset of thermal degradation, as shown in Figure 4.

The reaction enthalpic changes are measured during isothermal measurements, as shown in Figure 5. Or, if residual enthalpies are used, then an isotherm is followed by a similar ramp as the total enthalpy measurement, as shown in the chronogram in Figure 6 and the thermogram in Figure 7. Although the value is reported as the degree of cure, it should be understood that the actual degree of cure is not necessarily equal to this value since an assumption has been made that the total enthalpy represents complete or 100 % conversion.[20]

The reaction rate $d\alpha/dt$ is related to the heat flow dH/dt by the relationship

$$\frac{d\alpha}{dt} = \frac{1}{\Delta H_{total}} \frac{dH}{dt} . \qquad (2)$$

The rate of the curing reaction can be determined from the isothermal data used to determine the degree of cure. Since the enthalpy change is plotted as a function of time, the rate of change in time dH/dt will represent the rate of the reaction.

Nonisothermal methods, utilizing a single temperature scan run to monitor reaction enthalpic change,[21] as in Figure 8 or using a series of scans with different rates,[22] as shown in Figure 9 are advantageous due to the shorter time to run the experiments and avoidance of estimation of the lost area at the beginning of the isothermals. However, nonisothermal experiments are generally less accurate than isothermal ones.[23]

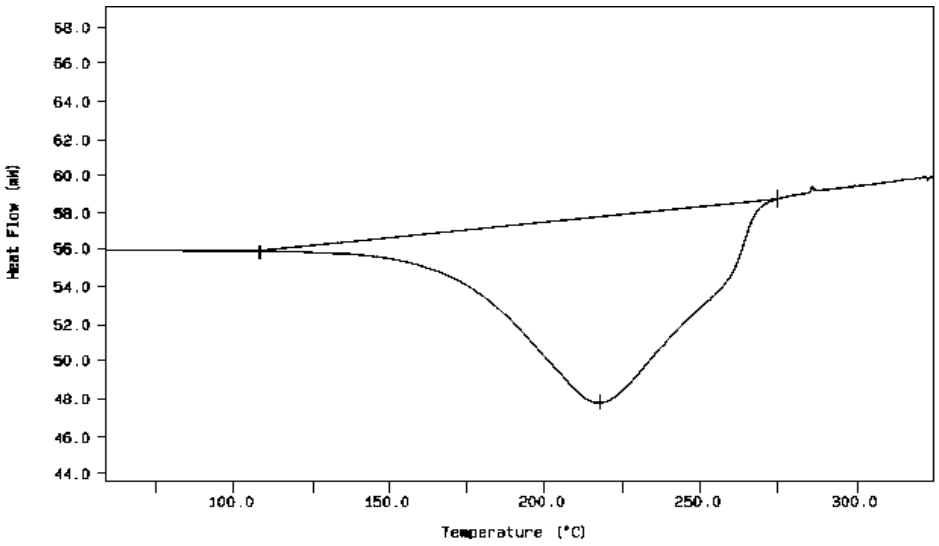

Figure 4: An example of a DSC thermogram showing the total ΔH from a slow temperature scan.

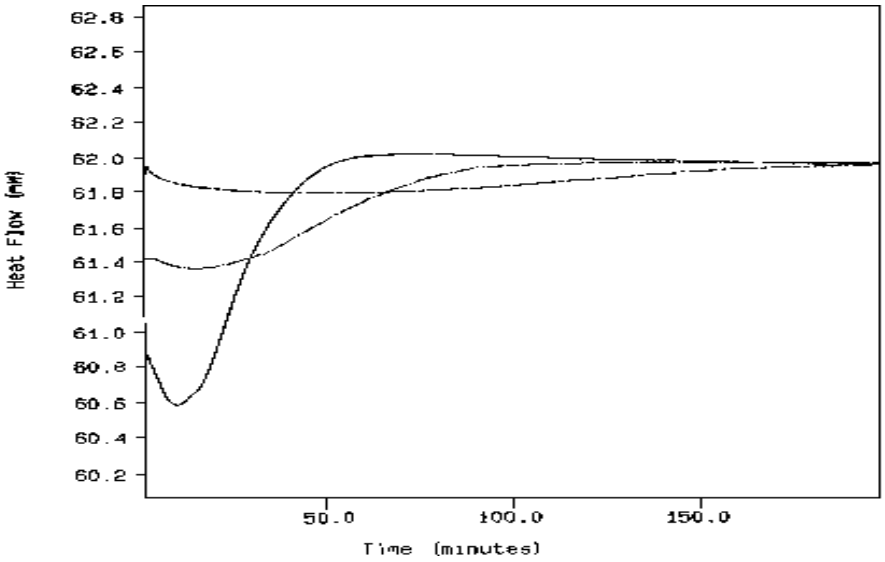

Fig.5. An example of a DSC thermogram, showing a series of isothermal measurements.

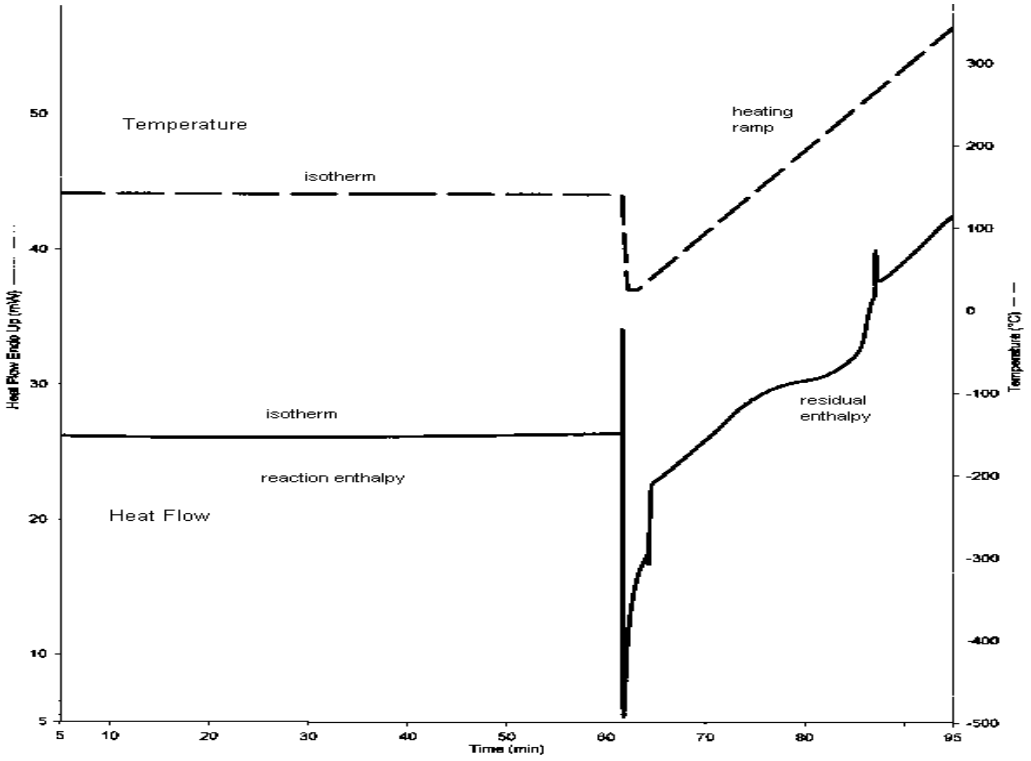

Fig. 6. A DSC chronograph showing the complete process of determining residual enthalpy, including a fast ramp to temperature, a hold time at the isothermal temperature, a quench to low temperature and a slow temperature scan.

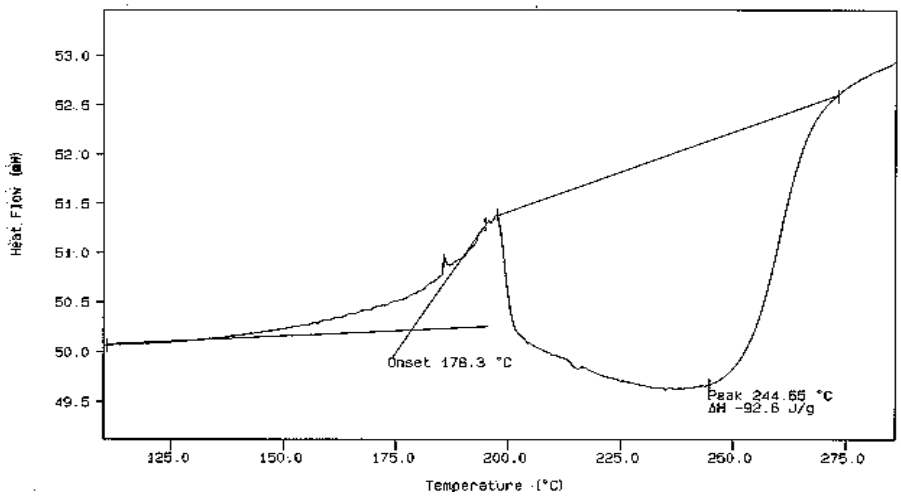

Fig. 7. An example of a DSC thermogram, showing the measurement of residual cure, or residual enthalpy in a partially cured sample; in this case the sample was cured for 200 minutes at 160°C.

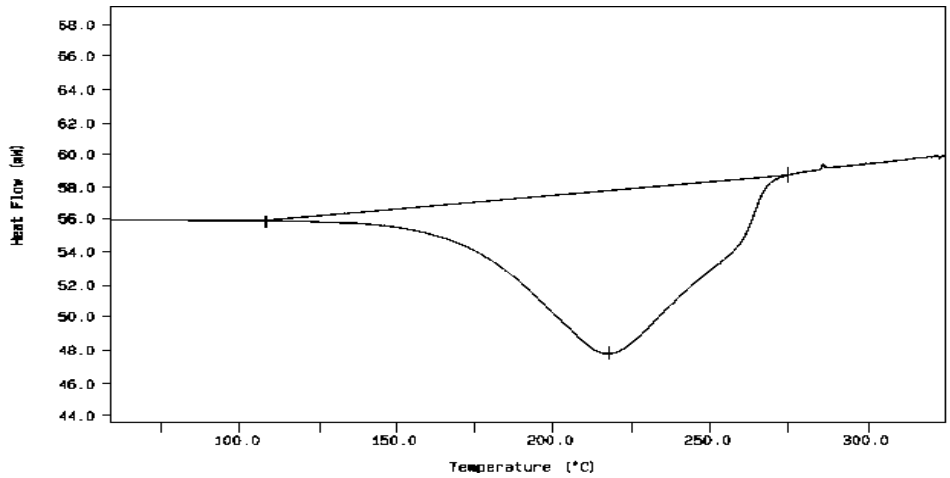

Fig. 8. An example of a DSC thermogram of a ΔH scan (at 5 K/min) from which the rate of the reaction can be calculated using a single scan model.

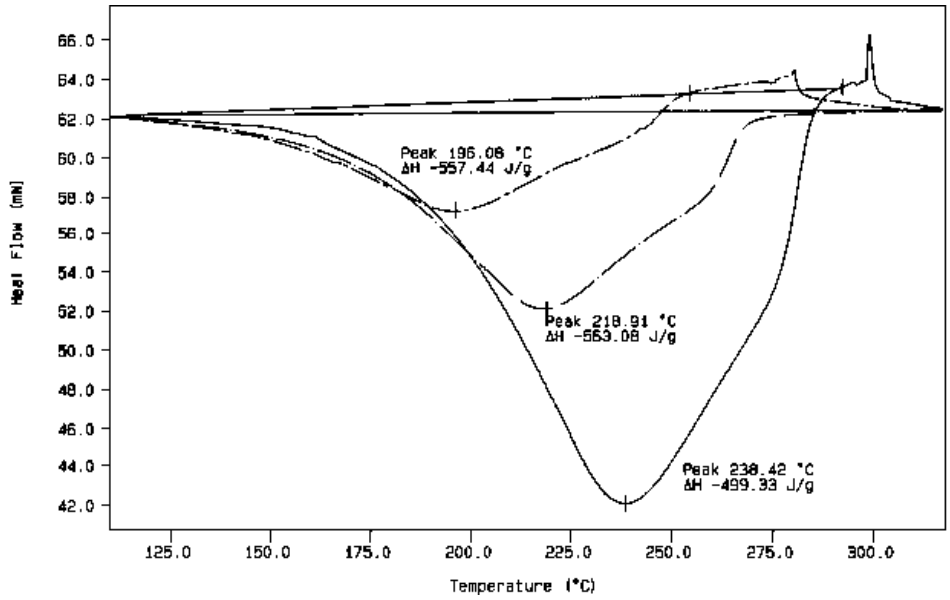

Fig. 9. A series of DSC thermograms at different scanning rates (5, 10 and 20 K/min), from which a time dependent rate can be calculated.

3. MOLECULAR WEIGHT, SEGMENT MOBILITY, CROSSLINK DENSITY

Epoxy curing involves an increase in both linear molecular weight and crosslink density, both of which result in reduced chain segment mobility. Increasing the linear molecular weight or crosslink density of a polymer chain increases the position of the glass transition temperature T_g - as shown in Figure 10. Many thermosetting polymer systems exhibit a relationship between the T_g and the degree of chemical conversion.[24] Most amine-cured epoxy systems exhibit a linear relationship, which implies that the change in molecular structure with conversion is independent of the cure temperature.[25] Such a T_g shift, in many circumstances, gives better resolution than exothermic enthalpy changes,[26] especially at high and low degrees of cure.

Descriptions of the shift as a function of chemical structure,[27-31] as well as extensive theoretical models based on either free volume[32-39] or time-dependent relaxation[40-50] abundant in the literature. Evidence for free volume models comes primarily from the pressure dependence of T_g in both Thermomechanical Analysis (TMA)[51] and DSC[52] measurements, whereas relaxation effects can be seen in the frequency dependence of Dynamic Mechanical Analysis (DMA) measurements,[53] as well as the effect of scanning rate in most thermal analysis techniques.[54] The T_g can be measured by a variety of techniques, each with certain advantages and disadvantages depending on the material and conditions. Comparisons of techniques show that while sensitivity to transitions vary,[55] the value of the T_g is similar given appropriate conditions.[56]

3.1 Differential Scanning Calorimetry

The most convenient and generally most accurate method for determining the T_g of polymers is DSC.[57] The T_g is taken as the temperature at the inflection point (peak of derivative curve)[58] of the baseline shift in heat flow or as the temperature at the half height shift in baseline heat flow. In situations where the T_g is distorted or masked by other events, like curing exotherms or enthalpic relaxations, the T_g may be determined by the onset, but results should be noted as onset values to avoid confusion. For consistency in reporting, an ASTM standard has been established.[59]

The shift in baseline heat flow associated with the glass transition is a result of the difference in heat capacity between the rubber and the glass.[60] Since this shift is an effect of the heat capacity change, resolution of the glass transition can be increased by calculating and plotting the constant pressure heat capacity, C_p. The C_p curve is calculated by comparing the heat flow (or differential power supplied), a baseline, and a reference material, usually sapphire, as described in an ASTM standard.[61] A power-compensation DSC has a long term energy calibration stability, hence the sapphire measurement is unnecessary if the curve is available in the software or has been run before, provided that the DSC has been properly calibrated using a high purity heat of fusion standard such as indium.[62]

The versatility of DSC to measure both exotherms and T_gs is also a limitation; when measuring an uncured or a partially cured thermoset, a residual exotherm follows the T_g being measured sometimes even overlapping it - as shown in Figure 11.

Accurate T_g calculations require stable baselines before and after the transition and the curing exotherm interferes with the upper baseline. In these cases, the T_g can only be determined as the onset.

3.2 Temperature-Modulated DSC

An alternative to the measurement of C_p is Temperature-Modulated DSC (TMDSC). TMDSC utilizes a modulated temperature ramp, much like dynamic mechanical analysis

uses a dynamic force and dielectric relaxation analysis uses an alternating current. TMDSC is a derivative of an earlier technique, Alternating Current (AC) Calorimetry.[63] AC Calorimetry utilizes an oscillating heating ramp, accomplished by the use of an auxiliary pulsed heat source (usually a chopped laser) over the linear programmed heating ramp, to measure the C_p during the single run experiment.[64] Analogous to Dynamic Mechanical Analysis (DMA) and Dielectric Analysis (DEA), TMDSC mathematically deconvolutes the response into two types of signals, an in-phase and an out-of-phase response to the modulations, as well as producing an average heat flow, which is analogous to the DSC signal using a linear heating ramp. There are two primary methods of performing TMDSC, sinusoidal and square wave modulation.

The first method, introduced by Reading[65] utilizes a sinusoidal modulation superimposed over the traditional linear heating ramp or isotherm, shown in Figure 12. The other method, introduced by Schawe[66] utilizes square wave modulations, shown in Figure 13. The two methods can be described by a single temperature function

$$T(t) = T_0 + \beta_0 t + (4/\pi)T_a[\ (\sin(\omega_0 t)/1^2) - (\sin(3\omega_0 t)/3^2) + (\sin(5\omega_0 t)/5^2) - \ldots.] \qquad (3)$$

where T_0 is the initial temperature, β_0 is the underlying heating rate, T_a is the amplitude of the temperature modulation and ω_0 is the angular frequency.[67] In the special case of sinusoidal modulation, the first harmonic would dominate the series.

Although the modulations are related and can be described by a single function (Equation 3), the methods of evaluation of the signal developed by Reading and Schawe are quite different. Both methods use a Fourier transform to produce an average heating rate q_{av}, an average heat flow h_{av}, an amplitude of heating rate A_q, an amplitude of heat flow A_h and a phase angle between the heating rate and heat flow φ.[68] However, Reading and Schawe use these values in different ways to calculate the values of the components.

Reading's technique[69] produces three values. The total heat flow ($H_T = h_{av}/q_{av}$) is usually expressed as the total heat capacity (C_p^T) representing the response to the overall average heating ramp, which is similar to what would be observed in linear DSC heat capacity measurements. The "reversing" component ($C_p^{rev} = A_h/A_q$) represents the ratio of the amplitude of the heat flow to the amplitude of the heating rate. These two signals are subtracted to yield the "non-reversing" component ($C_p^{nrv} = C_p^T - C_p^{rev}$). The reversing component represents thermally reversible events, such as T_gs and meltings, whereas the non-reversing component will represent thermally irreversible events, including relaxations, crystallizations and curing exotherms.

Schawe's technique[70-72] uses a linear response approach, which includes a dependence on the phase lag between the signal and response. His approach also begins with the total heat capacity ($C_p^T = h_{av}/q_{av}$) and includes a C_p value calculated as the ratio of the heat flow amplitude to the heating rate amplitude. However, his value is called the complex heat capacity ($C_p^* = A_h/A_q$). The reason for the difference is that from this value, he proposes a separation of the complex heat capacity (C_p^*) into two components, real and imaginary :

$$C_p^* = C_p' + iC_p'' \qquad (4)$$

with C_p' representing the real, in-phase component, termed storage heat capacity, and C_p'' representing the imaginary, out-of-phase component, called loss heat capacity. The two values are calculated using the phase angle φ between the signal and response :

$$C_p' = C_p^* \cos\varphi \qquad (5)$$

$$C_p'' = C_p^* \sin\varphi \qquad (6)$$

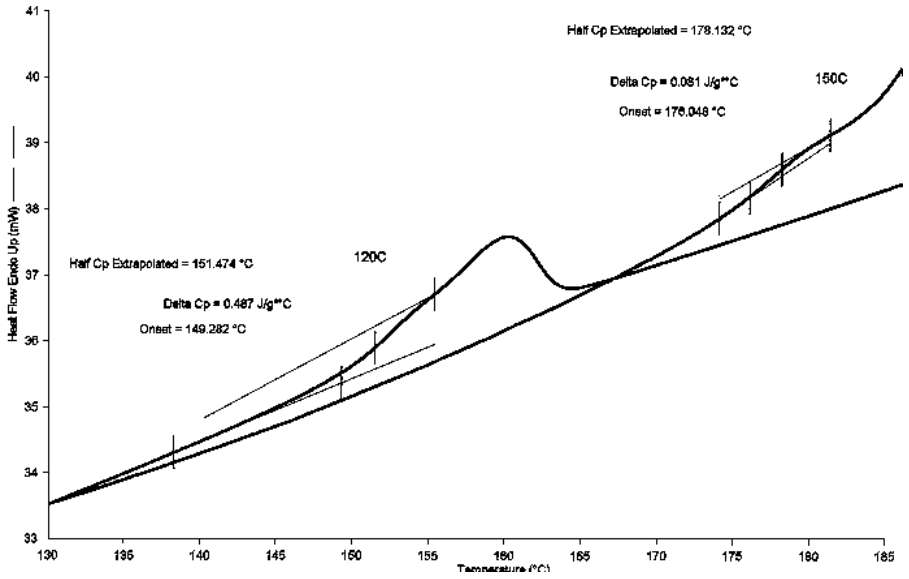

Fig. 10. A DSC thermogram showing the difference in T_g of two identical samples cured at different temperatures.

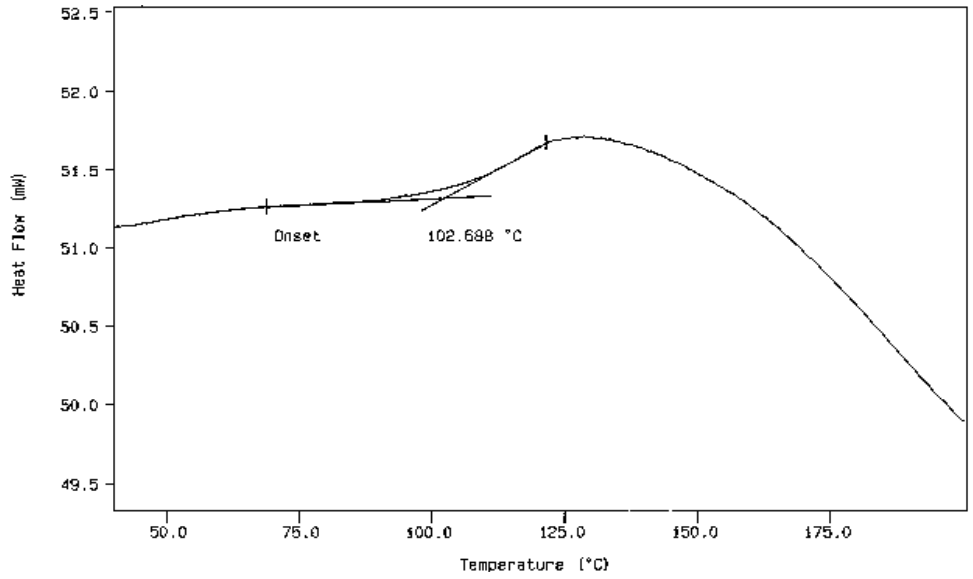

Fig. 11. An example of a DSC thermogram with the curing exotherm occurring right after the T_g , distorting both measurements.

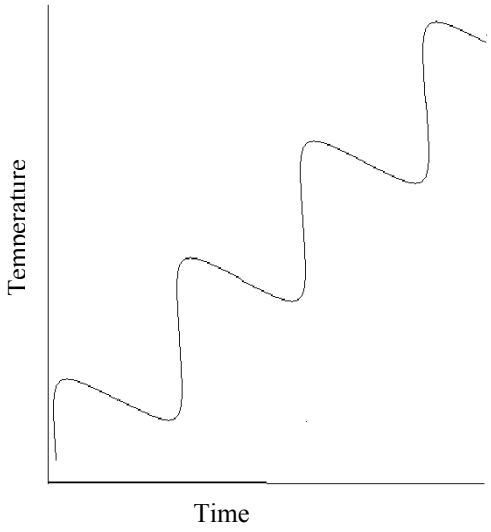

Fig. 12. Sine wave temperature modulations (Reading).

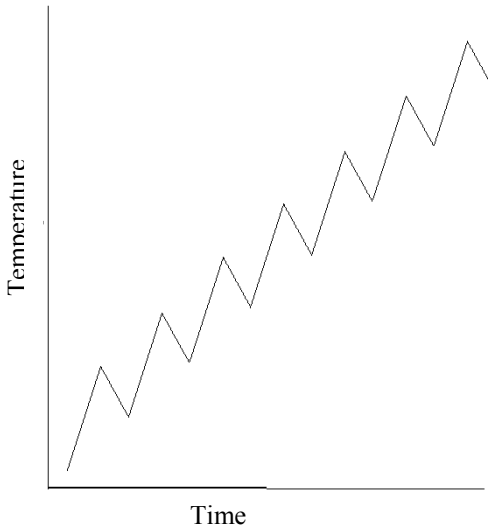

Fig. 13. Square wave temperature modulations (Schawe).

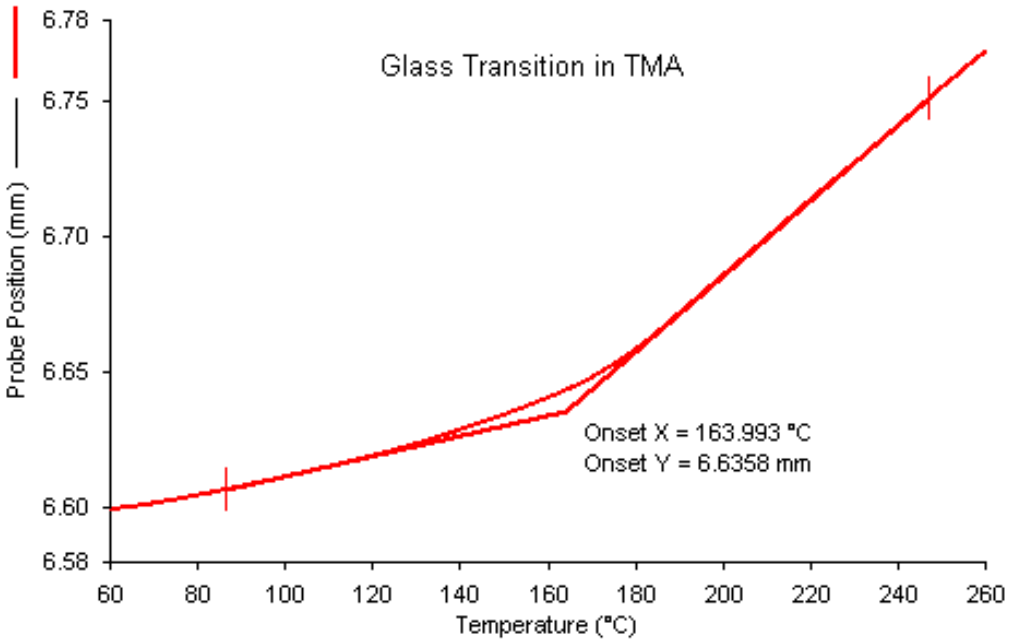

Fig. 14. An example of a TMA thermogram showing the change in slope of the expansion, or linear displacement with temperature, with the onset of change in slope representing the T_g.

Hutchinson and Montserrat[73] have evaluated the various types of modulations based on sine and square waves and the methods of evaluation and constructed a single parameter model to explain and predict the signals generated in TMDSC.

As in DMA and DEA measurements, the storage signal will include the elastic or in-phase response of the material, which in this case will be the molecular level responses, including glass transitions and meltings. The loss signal represents viscous or out-of-phase events, which are the kinetic effects, such as stress relaxations, crystallizations and curing. The total heat capacity is the average signal, which is equivalent to the heat capacity signal produced by traditional DSC.

3.3 Thermomechanical Analysis

The T_g can also be measured accurately using thermomechanical analysis (TMA). TMA is the measurement of changes in linear or volumetric dimension as a function of temperature or time.[74] The T_g appears as an abrupt increase in slope in the linear thermal expansion curve**,** shown in Figure 14, with the T_g indicated as the calculated onset of the change in slope, as described in an ASTM standard.[75] Volumetric measurements are performed using a dilatometry cup fitted with a movable piston. The volume changes are directly proportional to the linear movement of the piston, by simple geometry. In addition to the sensitivity of the technique to the T_g,[76] the linear or volumetric change in dimension with temperature gives insight into molecular structure.[77] The slope of the dimensional change as a function of temperature is the isobaric thermal expansivity or the ASTM[78] defined "linear or volumetric coefficient of thermal expansion" (LCTE or VCTE).

Modern TMA instruments employ a low voltage differential transducer (LVDT) to measure dimensional changes against the probe tip, producing resolution of linear changes in micro- to nanometer scale. A TMA instrument must be calibrated for height using dimensionally precise quartz standards, as well as temperature from the melting (collapse) of a high purity standard such as indium, as described by an ASTM standard.[79]

3.4 Dynamic Mechanical Analysis

Epoxies undergo changes in mechanical behavior as a function of cure. In addition to the shift in T_g, there are changes in the viscoelastic behavior[80] due to both polymerization and crosslinking. Dynamic Mechanical Analysis (DMA) instruments allow the application of a dynamic force in addition to the static force of TMA, just as TMDSC allows a modulated temperature signal over the linear temperature ramp of DSC. As shown in Figure 15, the phase lag between the applied dynamic force and the response yields a complex modulus, which can be mathematically separated into storage or in-phase elastic response E' and loss or out-of-phase viscous response E".

$$E^* = E' + iE'' = \sigma^* / \varepsilon^*. \quad (7)$$

$$\tan \delta = E''/E' \quad (8)$$

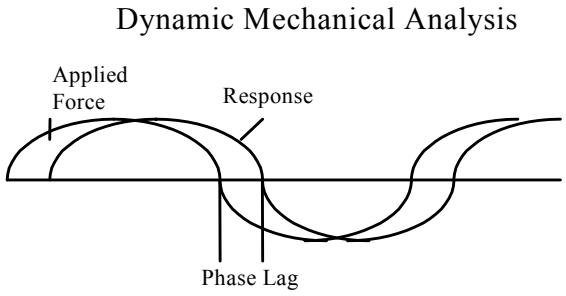

Fig. 15. Signal – Response for DMA measurements

The T_g can be measured accurately using dynamic mechanical analysis (DMA), which can in the case of highly filled or highly crosslinked polymers give better resolution and more information than DSC[81] and better reproducibility than older techniques, such as Vicat softening[82] and deflection[83] temperature

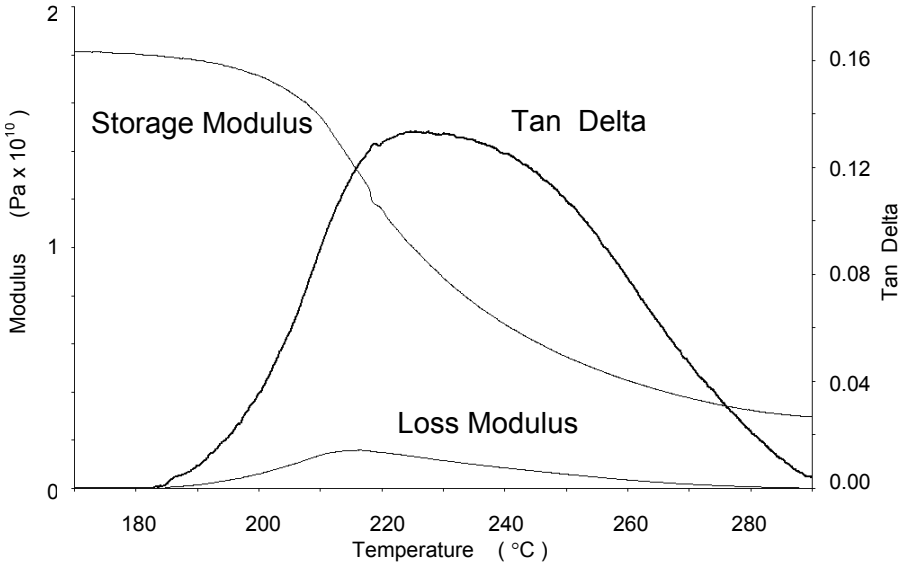

Fig. 16. A DMA thermogram using 3 point bending fixtures, showing all the signals used to calculate the T_g.

standards.[84] The T_g in a DMA measurement is generally taken as the peak in tangent delta,[85] but ASTM[86] recommends the peak in the loss modulus. Other methods include the inflection point or the half height value of the drop in storage modulus (E'), the onset of the drop in storage modulus, the onset of increase in loss modulus and the onset of the increase in tangent delta. A DMA thermogram is shown in Figure 16 with storage and loss moduli and tangent delta shown.

DMA (and TMA) measure dimensional changes and force responses using a variety of fixtures, each with specific applications and benefits. Applications include tensile, compression or expansion (linear and volumetric), flexural and shear.[87] Specialized techniques for shear measurements include torsional pendulum,[88] torsional braid analysis (TBA)[89] and torsional impregnated cloth analysis (TICA).[90] A DMA instrument must be calibrated for temperature, height and force. The temperature calibration is described by ASTM[91] using the melting temperature of a high purity standard. Height is determined using a quartz height standard. Force motor calibration is performed by balancing standard weights.

3.5 Thermally Stimulated Depolarization

Another method to measure the change in T_g and chain segment mobility during the curing process is based on thermally stimulated currents (TSC).[92] TSC is basically a low frequency (10^{-2} to 10^{-4} Hz) dielectric relaxation study.[93] TSC can be performed in either polarization (TSP) or depolarization (TSD) mode. TSC involves the polarization of electrets,[94] or dipoles within the polymer chain, making it very sensitive, even in copolymers,[95] highly crosslinked thermosets and filled composites. The sensitivity of TSC, specifically TSD, to molecular motion[96] and chain segment mobility yields well resolved T_g measurements,[97,98] in many cases, better resolved than DSC. Also, TSC experiments are not affected by mechanical effects like gelation as DMA is. TSC, especially TSD, measurements exhibit a time dependence, which can be measured as the characteristic

Debye[99] relaxation time, which is analogous to the DMA retardation or phase lag time.[100-105] A series of relaxation times[106] can be used to calculate the compensation point, which is the convergence of the frequency dependent relaxation times, much like extrapolation to zero heating rate in DSC or zero shear in DMA. TSP measures the polarization or absorption of charge by the polymer as a function of time or temperature, whereas TSD studies the depolarization or release of stored charge in a polarized sample. TSD is more useful in curing studies than TSP, hence emphasis is on TSD. Shifts in T_g as a function of conversion are performed in a similar fashion as shifts by DSC. Samples are cured at a certain temperature for a certain time, then quenched and the T_g determined during a controlled heating ramp, with T_g values plotted as a function of curing conditions (time and temperature).

In TSD a sample is quickly heated to a poling temperature where an electric field of predetermined strength is applied through parallel plates for a specific time. For thermosets, the poling temperature will be at the curing temperature and the poling time will be a part of the curing time. After poling, the sample is quenched to a relatively low temperature maintaining the electric field. At the selected low temperature, the electric field is discontinued and the circuit is shorted to dissipate any residual static charges. The sample is heated from this low temperature to a temperature higher than the poling temperature at a slow, controlled rate and any current discharged is measured using a sensitive picoammeter (sensitive to 10^{-15} Amperes or 10^7 electrons per second), and plotted against temperature. The TSD temperature program is depicted graphically in Figure 17. A typical TSD current thermogram is shown in Figure 18.

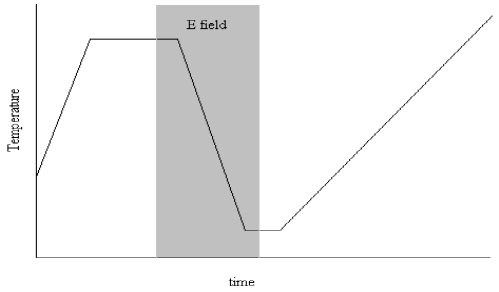

Fig. 17. Temperature program in TSD, with applied electric field shaded.

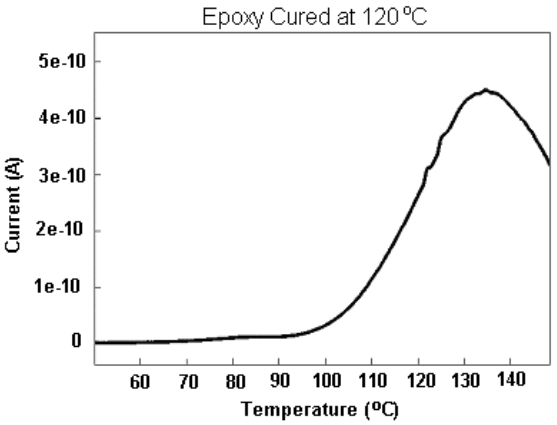

Fig. 18. TSD plot of discharge current as a function of temperature.

4. CHEMOVISCOSITY

The conversion induced change in viscosity, known as chemoviscosity, can be used to monitor conversion (analogous to T_g shift) and the change of physical state.[107] Since viscosity η describes a material's resistance to flow, it is defined as the ratio of shear stress τ to shear strain rate $d\gamma/dt$,

$$\eta = \frac{\tau}{(d\gamma/dt)} \quad . \qquad (10)$$

Viscosity measurements are performed routinely on liquids using a variety of methods, including capillary, concentric cylinder, cone and plate and many other viscometers. These techniques are well suited to measurements of liquids from low viscosity fluids, such as water (10^{-3} Pascal seconds) to higher viscosity ones, such as syrup (10^2 Ps), and even some polymer melts (10^2 to 10^7 Ps). However, measurment of very high viscosity materials from heavy pitch

(10^9 Ps) to window glass (10^{21} Ps) is beyond the range of most shear measurements. These high viscosity materials can be studied using DMA. However, DMA measures mechanical or Young's modulus E, rather than the shear modulus required for viscosity computation. Young's modulus E is related to shear modulus G_s by either the Poisson ratio ν[108] or the bulk modulus K_B,[109] given by

$$E = 2G_s(1 + \nu) = 3K_B(1 - 2\nu) \quad (10)$$

The Poisson ratio, also called the lateral strain contraction ratio, relates the change in lateral strain to the longitudinal strain.

From the moduli and the frequency ω of the measurements, the complex viscosity η^* can be calculated. It can be similarly separated into storage and loss components:

$$\eta^* = \eta' - i\eta'' = E^*/i\omega$$

$$= \frac{[(E')^2 + (E'')^2]^{1/2}}{\omega} \quad (11)$$

$$\eta' = E''/\omega \quad (12)$$

$$\eta'' = E'/\omega \quad (13)$$

The frequency of the dynamic signal has a large effect on the response, as depicted in Figure 19.

A single frequency series of isothermal DMA measurements of complex viscosity as a function of time, shown in Figure 20, exhibits the characteristic changes happening during a curing cycle. The epoxy prepreg is heated quickly to the isothermal temperature resulting in a temperature-dependent drop in viscosity. The minimum viscosity will generally be a function of the isothermal temperature, provided that no significant reaction has occurred, that is provided that the heating rate is faster than the time scale of the reaction onset. Of course, the value of the minimum viscosity will be determined by the molecular structure of the components of the prepreg and the effect of the overall mixture. However, usually the relative viscosities (relative to other isotherms) are used, so that the absolute value is not important in kinetics calculations. After the minimum viscosity, the reaction will proceed, increasing the molecular weight and the relative viscosity. This increase in viscosity, analogous to the rise in T_g used in previous models, is proportional to the increase in molecular weight, and thus the kinetics of the reaction.[110]

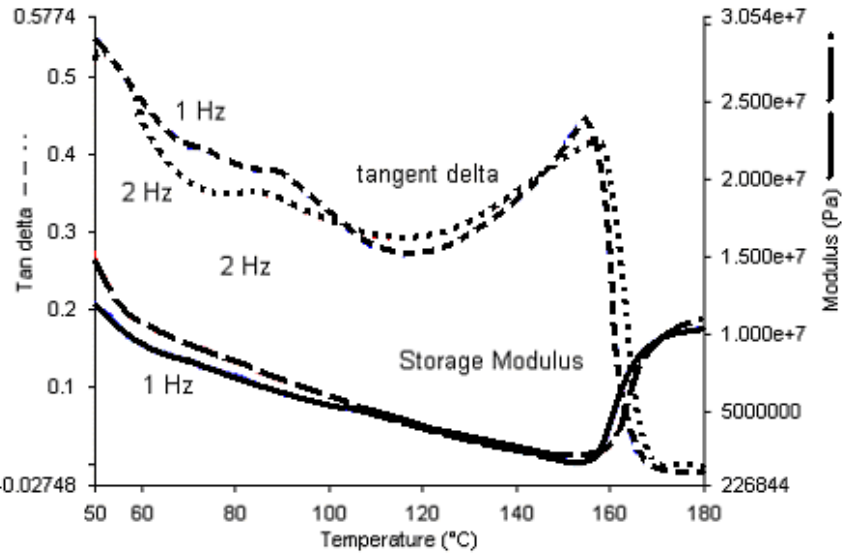

Fig.19. A series of 3-point bending DMA thermograms taken at different frequencies (1 and 2 Hz), showing the response as a function of frequency.

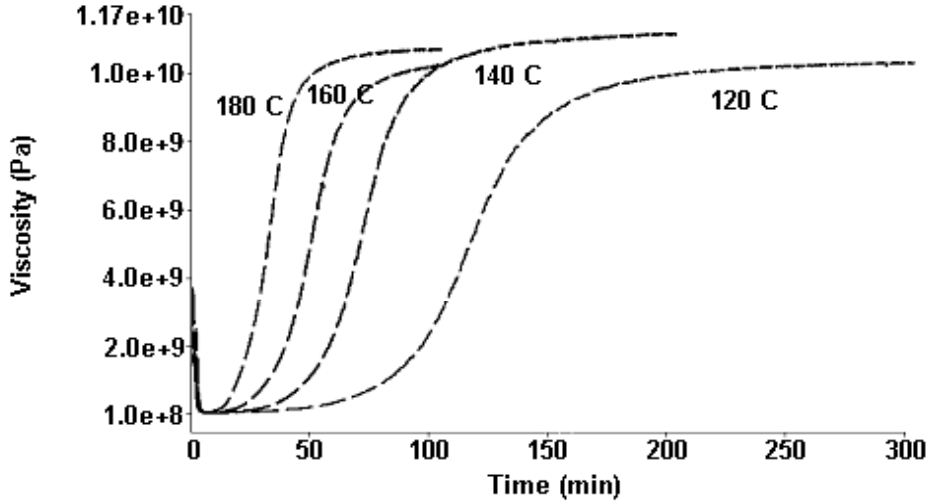

Fig. 20. A series of isothermal 3-point bending DMA plots of the change in complex viscosity as a function of time.

5. GELATION

Gelation refers to the point during the curing reaction where the molecular weight approaches the maximum, usually assumed to be infinite. That is, all monomers are connected to the network by at least one chemical bond. While gelation is a microscopic effect, it produces macroscopic effects. Microscopic gelation refers to the definition of the gelation phenomenon just provided. Since it occurs at a defined point in polymerization, it will occur at a specific degree of conversion.

Microscopic gelation is difficult to measure since the measurable properties would be solubility and molecular weight. However, the consequence of exceeding the microscopic gel point, is macroscopic gelation, which is much easier to measure. The macroscopic gel point is a mechanical property and can be identified by common thermal analysis techniques, including in-situ testing. Beyond gelation, there is no increase in molecular weight, only an increase in crosslink density and a decrease in free chain segment length.[111]

Gelation does not significantly affect the chemical conversion or curing reaction, so it does not appear in DSC measurements.[112] However, it does have a large influence on the mechanical properties of the polymer. Gelation affects the stiffness (modulus), adhesion and general processability of thermosets and composite prepregs, so it is important from an industrial processing standpoint. Gelation appears in the complex modulus, tangent delta and complex viscosity of DMA measurements; however, as with many thermal events, there is no unequivocal definition at which point the gelation occurs. Gillham,[113] who first plotted gelation curves as part of overall time-temperature-transformation (TTT) diagrams developed with Enns,[114,115] defines it as the a peak in the tangent delta of a DMA isotherm; this was also adopted as an ASTM standard.[116] Others define it as the peak in loss modulus. Some define it by the onset or inflection point of the increase in the storage modulus, whereas others define it as the onset of the plateau of the maximum of the storage modulus. A common method has been to use the crossover point, which is where the storage and loss moduli cross, or are equal, and the tan delta is equal to unity. However, this has been shown to be inaccurate in many cases and can only be used as an approximate measure or as a reference conversion value for a particular system. This discrepancy lies primarily in the application for

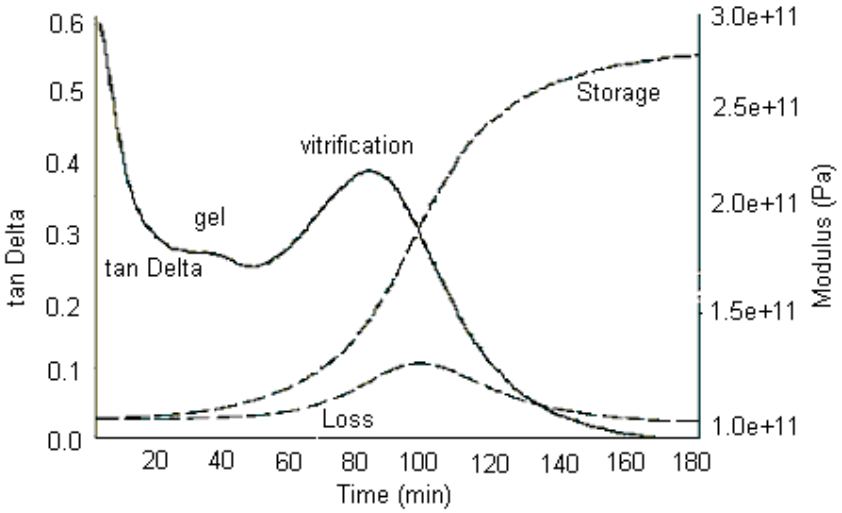

Fig. 21: A DMA isothermal 3 point bending plot showing tangent delta, from which gel point can be defined.

which the data is being used. Someone concerned with laminate adhesion would identify a different point than someone concerned with ensuring dimensional stability, and different than a researcher interested in characterizing the physical state of the material. The DMA isothermal plot in Figure 21 identifies the gel point using Gillham's terminology, i.e. the peak in tangent delta. As described earlier, DMA transitions exhibit a frequency dependence. However, since gelation is an isoconversion event, it is frequency independent. The gel point is therefore defined as the point where the tangent delta becomes frequency independent. However, this method requires many measurements at different frequencies. The gel point can be defined in terms of viscosity since it represents the maximum viscosity.

6. VITRIFICATION

Vitrification is defined as the point at which the molecular weight or cross-link density of the curing polymer exceeds that which is thermodynamically stable as a rubber, and the material undergoes a transition from a rubber to a glass at which point the reaction dramatically slows due to the reduced mobility of the reactants. The vitrification point can be measured using DSC, TMDSC and DMA.

Although vitrification is a thermal transition from a rubber to a glass and does appear in DSC measurements, the determination of the point and quantification of the shift in baseline heat flow or C_p usually occurs around the end of the curing (since it is a decrease in the reaction rate) and as such is usually masked by the curing reaction exotherm. This is one of the clearest applications of TMDSC since the curing exotherm appears in the loss C_p and vitrification appears in the storage C_p.[117,118] A series of isothermal TMDSC plots identifying the vitrification point are shown in Figure 22.

DMA has been used extensively to investigate the vitrification point, and continues to be the most common method. The first epoxy TTT diagram, proposed by Gillham and Enns,[119] was constructed primarily from torsional braid analysis (TBA), a specialized torsional DMA measurement. Gillham defines the vitrification in TBA and DMA measurements as the highest tangent Delta peak below the melt, which usually corresponds to the maximum value of the storage modulus during an isothermal experiment. Measurement of vitrification in

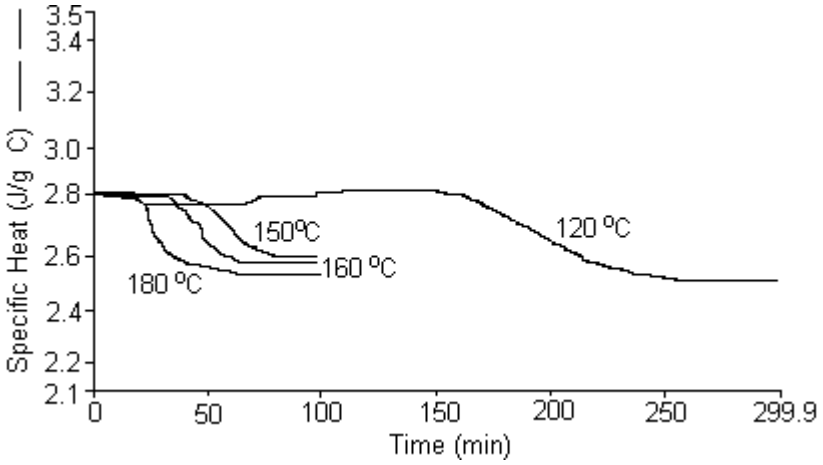

Fig. 22. TMDSC isotherms showing vitrification as half height drop in storage C_p.

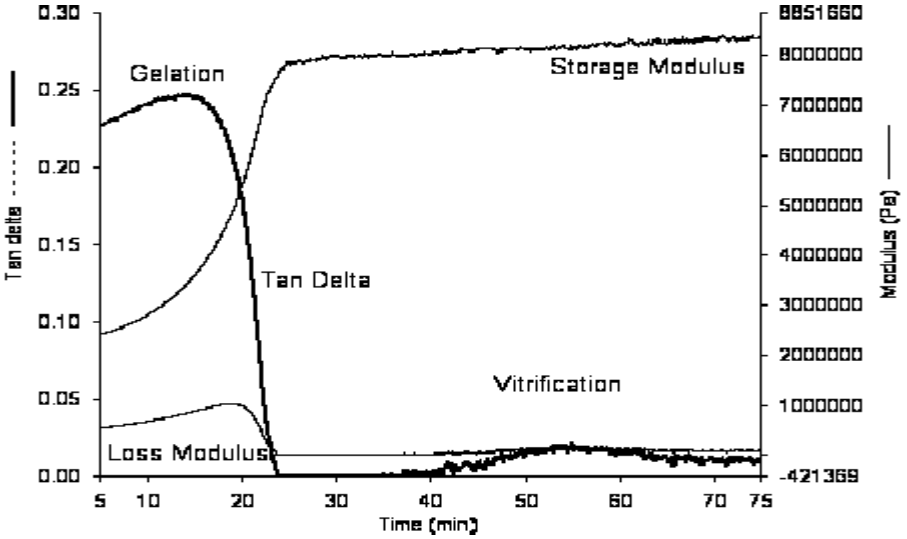

Fig. 23. A parallel plate DMA isotherm (160 °C), with vitrification defined by the second peak in tangent delta in time.

isothermal DMA and TBA studies are common. DMA isotherms showing vitrification points from parallel plate and 3-point bending modes are shown in Figures 21 and 23. Vitrification generally occurs when the increasing T_g equals the cure temperature.[120] Although the reaction dramatically slows, it is still significant until the T_g exceeds the cure temperature by 20 to 40 K.

7. THERMAL STABILITY

Thermogravimetric Analysis (TGA) is the measurement of weight loss as a function of temperature or time. A TGA instrument consists of a sensitive (typically $\pm$0.1 μg) microbalance monitoring the weight of a sample enclosed in a programmable oven. TGA is used extensively to study decomposition,

especially of multicomponent systems, including polymer blends, polymers with additives and reinforced and filled polymer composites. The offgassing of absorbed moisture or residual solvent can indicate the viscosity and gas permittivity of a sample in an indirect manner. Thermal stability or resistance to thermal degradation is related to the degree of cure, since the bond energies of aliphatic linkages tend to be higher than those of unsaturated structures. This relationship can be used to relate the kinetics of thermal decomposition to the curing reaction. TGA can be used to study the kinetics of either decomposition or chemical reactions involving the release of volatile by-products, i.e. condensation reactions. Kinetics can be evaluated using isoconversion data plots, activation energy calculated from the slope of initial reaction, varied heating rate analysis or a "model-free" method. TGA experiments can be performed in either oxidizing (O_2 or air) or non-oxidizing (N_2 or Ar) environments, depending on the reaction or decomposition being examined. A series of TGA decomposition thermograms are shown in Figure 24, with the method to calculate degradation temperature by onset illustrated in Figure 25.

TGA instruments must be calibrated for both temperature and weight. Weight calibrations are performed with standards which have been weighed to the desired accuracy (usually $\pm$ 0.1 μg) and will not react with moisture or oxygen in the air, as such platinum is a common standard. Temperature can be calibrated by two methods – fusable link or magnetic Curie temperature. The fusable link technique uses a small weight attached to the balance by a link made of a high purity standard which will result in a sudden weight loss at the melting point of the standard. The magnetic Curie temperature method uses the well known temperature-dependent magnetic properties of some metals and alloys. These materials exhibit a change in magnetism at a specific temperature, called the Curie point. The calibration is performed by placing a magnet above or below the standard in the TGA sample pan, where it will display an exceptionally high or low weight due to the magnetic field, until the temperature is raised to the Curie temperature. Materials and procedures have been recommended by the National Institute of Standards and Technology (NIST).[121]

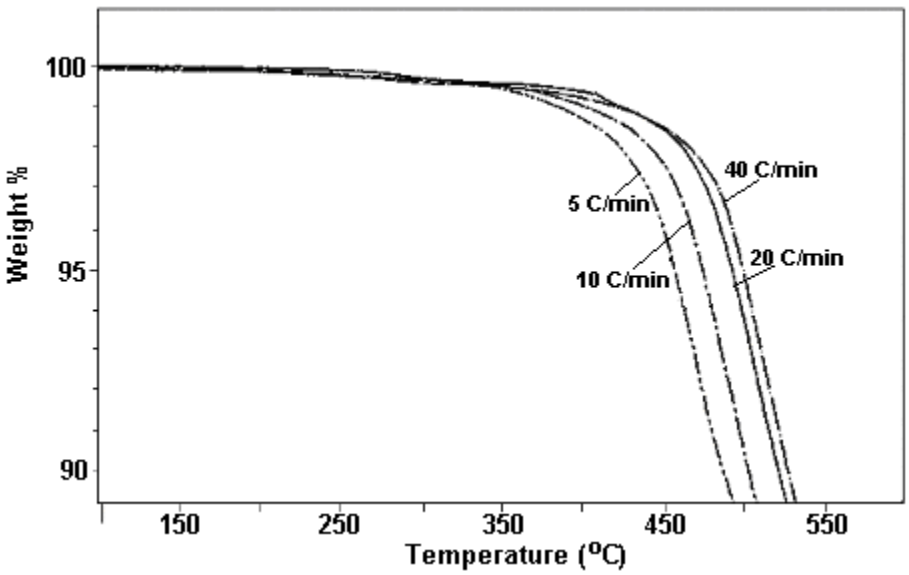

Fig. 24. A series of TGA decomposition thermograms at different scanning rates.

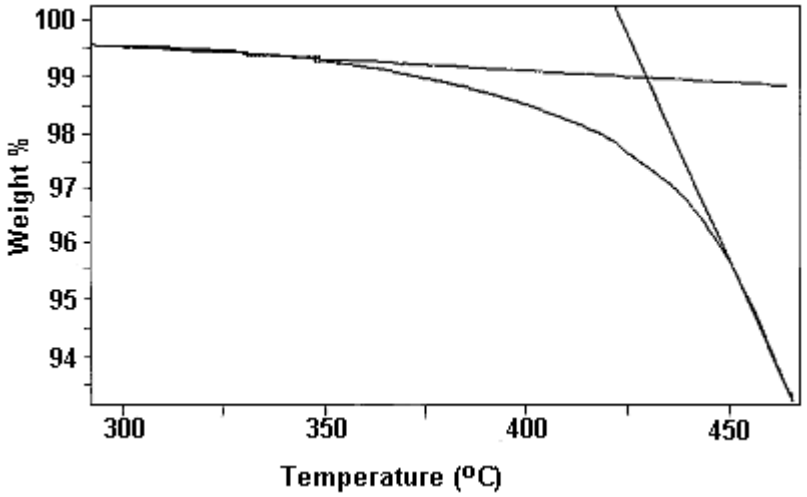

Fig. 25. TGA thermogram, showing method to calculate decomposition temperature from onset of weight drop.

8. ABBREVIATIONS/ ACRONYMS

AC	Alternating Current
ASTM	American Society for Testing and Materials
DEA	Dielectric (Relaxation) Analysis
DMA	Dynamic Mechanical Analysis
DSC	Differential Scanning Calorimetry
DTA	Differential Thermal Analysis
ICTAC	International Confederation for Thermal Analysis and Calorimetry
IUPAC	International Union of Pure and Applied Chemistry
LCTE	Linear Coefficient of Thermal Expansion
LVDT	Low Voltage Differential Transducer
NIST	National Institute of Standards and Technology
TBA	Torsional Braid Analysis
TGA	Thermogravimetric Analysis
TICA	Torsional Impregnated Cloth Analysis
TMA	Thermomechanical Analysis
TMDSC	Temperature-Modulated Differential Scanning Calorimetry
TSC	Thermally Stimulated Currents
TSD	Thermally Stimulated Depolarization
TSP	Thermally Stimulated Polarization
TTT	Time-Temperature-Transformation
VCTE	Volumetric Coefficient of Thermal Expansion

9. SYMBOLS

A	Amplitude
C_p	Specific Heat Capacity at Constant Pressure
C_p *	Complex Specific Heat Capacity at Constant Pressure
C_p ‘	Storage Specific Heat Capacity at Constant Pressure (Elastic Component)
C_p “	Loss Specific Heat Capacity at Constant Pressure (Viscous Component)
C_v	Specific Heat Capacity at Constant Volume
E	Young’s (Mechanical) Modulus
E*	Complex Young’s Modulus
E’	Storage Young’s Modulus (Elastic Component)
E”	Loss Young’s Modulus (Viscous Component)
g	gram
G	Gibbs’ Function
G_s	Shear Modulus
H	Enthalpy
dH/dt	Rate of Change of Enthalpy in Time
Hz	Hertz (cycles per second)
K_s	Bulk Modulus

P	Pascal (pressure unit)
q	Heat Quantity
s	Second (time unit)
S	Entropy
T	Temperature
T_g	Glass Transition Temperature
α	Degree of Conversion
δ	phase angle (usually given as tan δ)
ε	Mechanical Strain
γ	Shear Strain
η	Viscosity
η^*	Complex Viscosity
η'	Storage Viscosity (Elastic Component)
η''	Loss Viscosity (Viscous Component)
ν	Poisson's Ratio
φ	Phase Angle
σ	Mechanical Stress
τ	Shear Stress
ω	Angular Frequency

REFERENCES

1. B. Bilyeu, W. Brostow and K.P. Menard, *J. Mater. Ed.*, **21**, 281 (1999).
2. R. Vieweg, *Prog. Vac. Microbal. Tech.*, **1,** 1 (1972).
3. B. Wunderlich, *Thermal Characterization of Polymeric Materials (Second Edition)*, ed. E. Turi, Chapter 2, Academic Press, San Diego (1997) p. 206.
4. H. Le Chatelier, *Bull. Soc. Min. Crist.*, **10,** 204 (1887).
5. W. Nernst and E.H. Riesenfeld, *Ber. Deut. Chem. Ges.*, **36,** 2086 (1903).
6. B. Wunderlich, *Thermal Analysis*, Academic Press, San Diego (1990).
7. J.O. Hill, *Better Thermal Analysis and Calorimetry*, 3rd Edition, CPC Reprographics, Portsmouth, U.K. (1991).
8. P.K. Gallagher, *Thermal Characterization of Polymeric Materials (Second Edition)*, ed. E. Turi, Chapter 1, Academic Press, San Diego (1997) p.2.
9. M.A. Fox and J.K. Whitesell, *Organic Chemistry*, Jones and Bartlett Publishers, Boston (1994).
10. M.J. Richardson, *Developments in Polymer Characterization*, ed. J.V. Dawkins, Chapter 7, Applied Science Publishers LTD, London (1978) p.205.
11. S.L. Boersma, *J. Amer. Cer. Soc.*, **38**, 281 (1955).
12. D.J. David, *J. Thermal Anal.*, **3,** 1 (1971).
13. E.S. Watson, M.J. O'Neill, J. Justin and N. Brenner, *Anal. Chem.*, **36,** 1233 (1964).
14. M.J. O'Neill, *Anal. Chem.*, **36,** 1238 (1964).
15. R.F. Speyer, *Thermal Analysis of Materials*, Marcel Dekker, New York (1994).
16. T.J. Quinn, *Temperature*, Academic Press, San Diego (1990).
17. J.H. Flynn, *Analytical Calorimetry, Vol. 3*, eds. R.S. Porter, J.F. Johnson, Plenum Press, New York (1970) p.17.
18. W. Hemminger, *Calorimetry and Thermal Analysis of Polymers*, ed. V.B.F. Mathot, Chapter 2, Hanser, Munich (1994) p.17.
19. B. Fuller, J.T. Gotro and G.C. Martin, *Polymer Characterization*, eds. C. Craver and T. Provder, Chapter 12, American Chemical Society, Washington D.C. (1990) p.215.
20. J.P. Creedon, *Analytical Calorimetry, Vol. 2*, eds. R.S. Porter, J.F. Johnson, Plenum Press, New York (1970) p.185.
21. H.J. Borchardt and F. Daniels, *J. Amer. Chem. Soc.*, **79,** 41 (1956).
22. P. Peyser and W.D. Bascom, *Analytical Calorimetry, Vol. 3*, eds. R.S. Porter, J.F. Johnson, Plenum Press, New York (1970) p.537.
23. R.B. Prime, *Analytical Calorimetry, Vol. 2*, eds. R.S. Porter, J.F. Johnson, Plenum Press, New York (1970) p.201.
24. R.P. Chartoff, *Thermal Characterization of Polymeric Materials (Second Edition)*, ed. E. Turi, Chapter 3, Academic Press, San Diego (1997) p.484.
25. G. Wisanrakkit and J.K. Gillham, *Polymer Characterization*, eds. C. Craver and T. Provder, Chapter 9, American Chemical Society, Washington D.C. (1990) p.143.
26. M.J. Richardson, *Pure and Appl. Chem.*, **64,** 1789 (1992).
27. A.R. Katritzky, P. Rachwal, K.W. Law, M. Karelson and V.S. Lobanov, *J. Chem. Inf. Comput. Sci.*, **36,** 879 (1996).

28. A.T. DiBenedetto, *J. Polymer Sci., Polymer Phys.*, **25,** 1949 (1987).
29. H. Stutz, J. Mertes and K. Neubecker, *J. Polymer Sci., Chem.*, **31,** 1879 (1993).
30. H. Stutz, K.H. Illers and J. Mertes, *J. Polymer Sci., Phys.*, **28,** 1483 (1990).
31. J.M. Barton, *Polymer Characterization by Thermal Methods of Analysis*, ed. J. Chiu, Dekker, New York (1974).
32. J.C. Bauwens, *Failure of Plastics*, eds. W. Brostow and R. Corneliussen, Chapter 12, Hanser, Munich (1986) p.235.
33. B. Hartmann and M.A. Haque, *J. Appl. Phys.*, **58,** 2831 (1985).
34. V.L. Maksimov, *Polymer Sci.*, **36,** 955 (1994).
35. W. Brostow, *Makromol. Chem., Symp.*, **41,** 119 (1991).
36. J.P. Ibar, *J. Macromol. Sci.*, **16,** 61 (1979).
37. D. Chinn, S.B. Shim and J.C. Seferis, *J. Thermal Anal.*, **46,** 1511 (1996).
38. W. Brostow, J.V. Duffy, G.F. Lee and K. Madejczyk, *Macromol.*, **24,** 479 (1991).
39. W.H. Jo and K.J. Ko, *Polymer Eng. & Sci.*, **31,** 239 (1991).
40. S. Matsuoka, *Failure of Plastics*, Eds. W. Brostow and R. Corneliussen, Chapter 3, Hanser, Munich (1986) p.24.
41. D.W. Van Krevelen, *Properties of Polymers*, Third Edition, Elsevier, Amsterdam (1990).
42. C.L. Rohn, *Analytical Polymer Rheology*, Hanser, Munich (1995).
43. I.M. Ward, *Mechanical Properties of Solid Polymers*, Wiley, New York (1983).
44. J.J. Aklonis and W.J. MacKnight, *Introduction to Polymer Viscoelasticity*, Wiley, New York (1983).
45. J.D. Ferry, *Viscoelastic Properties of Polymers*, Wiley, New York (1980).
46. J. Mijović and B. Schafran, *SAMPE J.*, **26,** 51 (1990).
47. B.B. Sauer and P. Avakian, *Polymer*, **33,** 5128 (1992).
48. S.H. Dillman and J.C. Seferis, *J. Macromol. Sci.*, **26,** 227 (1989).
49. E. Marchal, *J. Chem. Phys.*, **96,** 4676 (1992).
50. J. Kubát and M. Rigdahl, *Failure of Plastics*, eds. W. Brostow and R. Corneliussen, Chapter 4, Hanser, Munich (1986) p.60.
51. P. Zoller, T.A. Kehl, H.W. Starkweather,jr. and G.A. Jones, *J. Polymer Sci., Phys.*, **27,** 993 (1989).
52. M.J. Richardson, *Calorimetry and Thermal Analysis of Polymers*, ed. V.B.F. Mathot, Chapter 6, Hanser, Munich (1994) p.169.
53. K.P. Menard, *Dynamic Mechanical Analysis*, CRC Press, Boca Raton (1999).
54. J.H. Flynn, *Analytical Calorimetry, Vol. 3*, eds. R.S. Porter, J.F. Johnson, Plenum Press, New York (1970) p.17.
55. H.R. O'Neal, S. Welch, J. Rogers, S. Guilford, G. Curran and K.P. Menard, *J. Adv. Mater.*, **26,** 49 (1995).
56. B. Cassel and B. Twombly, *Material Characterization by TMA*, eds. A.T. Riga and C.M. Neag, ASTM, Philadelphia (1991) p.108.
57. L.H. Sperling, *Introduction to Physical Polymer Science*, Wiley, New York (1986).
58. V.A. Bershtein and V.M. Egorov, *Differential Scanning Calorimetry of Polymers*, Ellis Horwood, New York (1994).
59. ASTM E1356-91, American Society for Testing and Materials, Philadelphia (1991).
60. Y.K. Godovsky, *Thermophysical Properties of Polymers*, Springer-Verlag, Berlin (1992).
61. ASTM E1269-90, American Society for Testing and Materials, Philadelphia (1990).
62. V.B.F. Mathot, *Calorimetry and Thermal Analysis of Polymers*, ed. V.B.F. Mathot, Chapter 5, Hanser, Munich (1994) p.105.
63. P. Sullivan and G. Seidel, *Phys. Rev.*, **173,** 679 (1968).
64. R. Viswenathan, *Analytical Calorimetry, Vol. 3*, eds. R.S. Porter, J.F. Johnson, Plenum Press, New York (1970) p.81.
65. M. Reading, D. Elliot and V. Hill, *Proc. N. Amer. Thermal Anal. Soc. Conf.*, **21,** 145 (1992).
66. J. Schawe and M. Marguilies, US Patent 5549387 (1996).

67. B. Gopalanarayanan, Ph.D. Dissertation, University of North Texas, Denton (1998).
68. J.M. Hutchinson and S. Montserrat, *Thermochim. Acta*, **304/305,** 257 (1997).
69. K.J. Jones, I. Kinshott, M. Reading, A.A. Lacey, C. Nikolopoulos and H.M. Pollock, *Thermochim. Acta*, **304/305,** 187 (1997).
70. J.E.K. Schawe, *Thermochim. Acta*, **270,** 1 (1995).
71. J.E.K. Schawe, *Thermochim. Acta*, **261,** 183 (1995).
72. J.E.K. Schawe, *Thermochim. Acta*, **260,** 1 (1995).
73. J.M. Hutchinson and S. Montserrat, *Thermochim. Acta*, **286,** 263 (1996).
74. C.M. Neag, *Material Characterization by Thermomechanical Analysis*, American Society for Testing and Materials, Philadelphia (1991).
75. ASTM E1545-95a, American Society for Testing and Materials, Philadelphia (1995).
76. R.E. Cuthrell, *J. Appl. Polymer Sci*., **12,** 955 (1968).
77. J.M. Powers and R.G. Craig, *Analytical Calorimetry, Vol. 3*, eds. R.S. Porter, J.F. Johnson, Plenum Press, New York (1970) p.349.
78. ASTM E228-95, American Society for Testing and Materials, Philadelphia (1995).
79. ASTM E1363-97, American Society for Testing and Materials, Philadelphia (1997).
80. J.D. Ferry, *Viscoelastic Properties of Polymers*, Wiley, New York (1980).
81. H. Mallela, M. Davis and K.P. Menard, *Proc. Ann. Tech. Conf. Soc. Plast. Engrs.*, **40,** 2276 (1994).
82. ASTM D1525-96, American Society for Testing and Materials, Philadelphia (1996).
83. ASTM D648-97, American Society for Testing and Materials, Philadelphia (1997).
84. M. Akay, J.G. Cracknell and H.A. Farnham, *Polymer & Polymer Comp.*, **2,** 317 (1994).
85. T.W. Wilson, R.E. Fornes, R.D. Gilbert and J.D. Memory, *Cross-Linked Polymers*, eds. R.A. Dickie, S.S. Labana, R.S. Bauer, Chapter 7, American Chemical Society, Washington D.C. (1988).
86. ASTM E1640-94, American Society for Testing and Materials, Philadelphia (1994).
87. B. Cassel and B. Twombly, *Am. Lab.*, Jan. (1991) p.34.
88. K. Schmieder and K. Wolf, *Kolloid Zeit.*, **127,** 65 (1952).
89. A.F. Lewis and J.K. Gillham, *J. Appl. Polymer Sci.*, **6,** 422 (1962).
90. C.Y.-C. Lee and I.J. Goldfarb, *Polymer Characterization*, ed. C. Craver, Chapter 3, American Chemical Society, Washington D.C. (1983) p.65.
91. ASTM E1867-97, American Society for Testing and Materials, Philadelphia (1997).
92. C. Bucci and R. Fieschi, *Phys. Rev.*, **12,** 16 (1964).
93. J.P. Ibar, P. Denning, T. Thomas, A. Bernes, C. deGoys, J.R. Saffell, P. Jones and C. Lacabanne, *Polymer Characterization*, eds. C. Craver and T. Provder, Chapter 10, American Chemical Society, Washington D.C. (1990) p.167.
94. J. Vanderschueren and J. Gasiot, *Thermally Stimulated Relaxation in Solids*, ed. P. Bräunlich, Springer-Verlag, New York (1979).
95. W. Brostow, B.K. Kaushik, S.B. Mall and I.M. Talwart, *Polymer*, **33,** 4687 (1992).
96. A.B. Dias, J.J. Moura-Ramos and G. Williams, *Polymer*, **35,** 1253 (1994).
97. B.B. Sauer, P. Avakian and G.M. Cohen, *Polymer*, **33,** 2666 (1992).
98. B.S. Hsiao and B.B. Sauer, *J. Polymer Sci., Phys.*, **31,** 917 (1993).
99. P. Debye, *Polar Molecules*, Chemical Catalog, New York (1929).
100. B.B. Sauer and P. Avakian, *Polymer*, **33,** 5128 (1992).
101. E. Marchal, *Polymer*, **32,** 297 (1991).
102. V. Halpern, *J. Phys. D: Appl. Phys.*, **25,** 1533 (1992).
103. V. Halpern, *J. Phys.: Condens. Matter*, **6,** 9451 (1994).
104. V. Halpern, *J. Phys.: Condens. Matter*, **7,** 7687 (1995).

105. V. Halpern, *Phys. Rev. B*, **56,** 377 (1997).
106. J.P. Ibar, P. Denning, T. Thomas, A. Bernes, C. deGoys, J.R. Saffell, P. Jones and C. Lacabanne, *Polymer Characterization*, eds. C. Craver and T. Provder, Chapter 10, American Chemical Society, Washington D.C. (1990) p.167.
107. R.J. Hinrichs, *Chemorheology of Thermosetting Polymers*, Amer. Chem. Soc., Washington D.C. (1983).
108. K.P. Menard, *Dynamic Mechanical Analysis*, CRC Press, Boca Raton (1999).
109. A.W. Birley, B. Haworth and J. Batchelor, *Physics of Plastics*, Hanser, Munich (1991).
110. A.Yousefi, P.G. Lafleur and R. Gauvin, *Polymer Compos*., **18,** 157 (1997).
111. K. Dušek and W.J. MacKnight, *Cross-Linked Polymers*, eds. R.A. Dickie, S.S. Labana, R.S. Bauer, Chapter 1, American Chemical Society, Washington D.C. (1988) p.2.
112. R.B. Prime, *Thermal Characterization of Polymeric Materials (Second Edition)*, ed. E. Turi, Chapter 6, Academic Press, San Diego (1997) p.1380.
113. J.K. Gillham and J.B. Enns, *Trends Polymer Sci.*, **2,** 406 (1994).
114. J.B. Enns and J.K. Gillham, *J. Appl. Polymer Sci.*, **28,** 2567 (1983).
115. J.B. Enns and J.K. Gillham, *Polymer Characterization*, ed. C. Craver, Chapter 2, American Chemical Society, Washington D.C. (1983) p.27.
116. ASTM D4473-90, American Society for Testing and Materials, Philadelphia (1990).
117. B. Bilyeu, W. Brostow and K. Menard, *Proc. Amer. Chem. Soc., Div. Polym. Mater. Sci. & Eng.*, **78,** 232 (1998).
118. B. Bilyeu, W. Brostow and K. Menard, *Proc. Ann. Tech. Conf. Soc. Plast. Engrs*., **45,** 2724 (1999).
119. J.K. Gillham, *AIChE J*., **20,** 1066 (1974).
120. J.K. Gillham, *Polymer Eng. and Sci*., **26,** 1429 (1986).
121. P.D. Garn, O. Menis and H.G. Wiedemann, *Thermal Analysis*, ed. H.G. Wiedemann, Birkh⊙eser, Basel (1980).

This page intentionally left blank